Pulse Formation on the Anode of Frisch-Gridded Ionization Chamber

Jaksybekov A., Svetov L., Sidorova O., Zeynalov Sh.

Joint Institute for Nuclear Research, Dubna, Russia

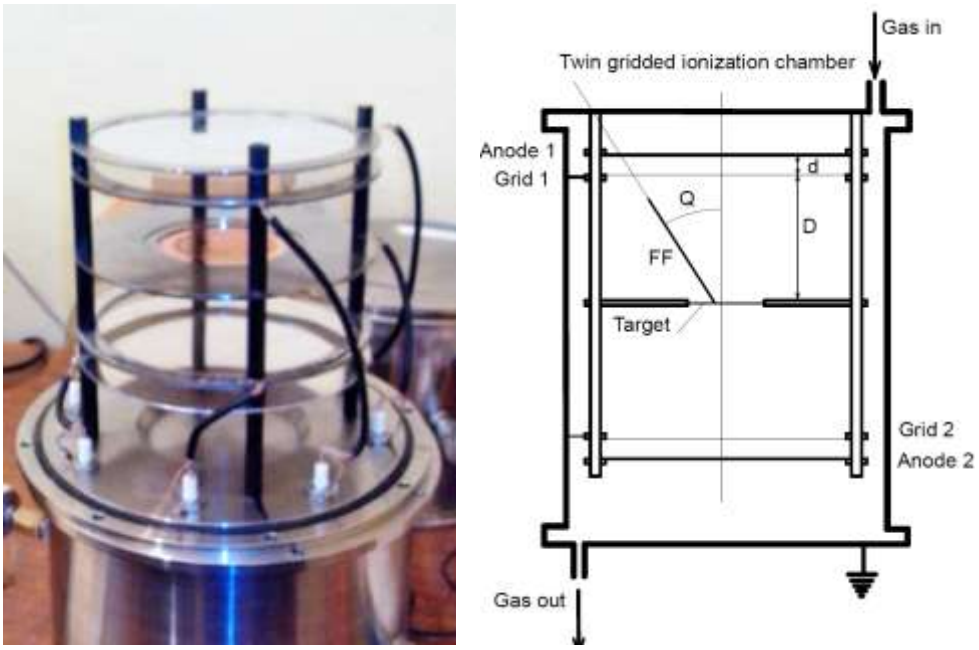

Figure 1. Photograph and scheme of the Twin Frisch-Gridded Ionization Chamber.

Application of Shokley-Ramo theorem to a TGIC

The general method to calculate induced charge on electrodes due to the motion of charge carriers in a detector makes use of the Shockley-Ramo theorem [1] and the concepts of the **weighting field** and **weighting potential**. The theorem states that the instantaneous current induced on a given electrode is equal to $i = q\bar{v}E_0$, where q is the charge of the carrier, $\bar{v}$ is its velocity, and E_0 is called the weighting field. Another way of stating the same principle is that the induced charge on the electrode is given by the product of the charge on the carrier multiplied by the difference in the weighting potential from the beginning to the end of the carrier path $Q=q\Delta\Phi$. To find this weighting potential as a function of position, one must solve the Laplace equation for the geometry of the detector, but with some artificial boundary conditions:

- The voltages on all other electrodes are set to zero.
- The voltage on the electrode for which the induced charge is to be calculated is set equal to unity.
- Even if a trapped charge is present within the detector volume, it is ignored in the calculation.

The solution under these conditions gives the weighting potential, and its gradient is the weighting field. The weighting potential is not the actual electric potential in the detector, but instead serves as a convenience that allows simple determination of the induced charge on

the electrode of interest by taking differences in the weighting potential at the start and end of the carrier motion.

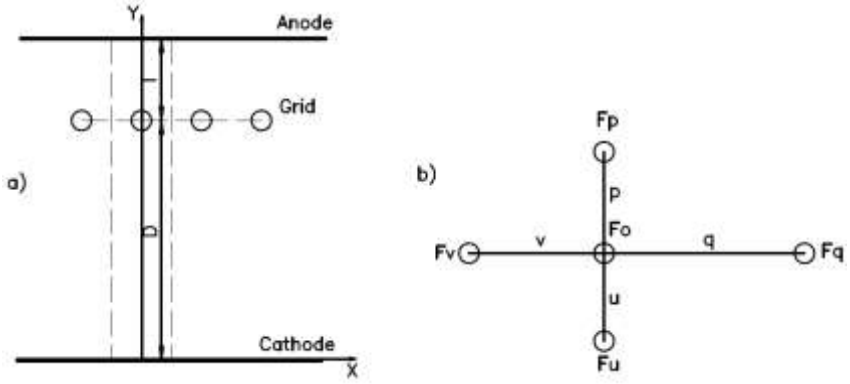

Figure 2. a) Area, confined by dashed lines, where the Laplace equation solved with periodical Dirichlet boundary conditions. b) generalized finite difference scheme demonstrating how the second order derivatives were calculated at the grid node F_0 using adjacent nodes F_q , F_p , F_p and F_v. Everywhere instead of the close vicinity of grid p=q=v=u=h.

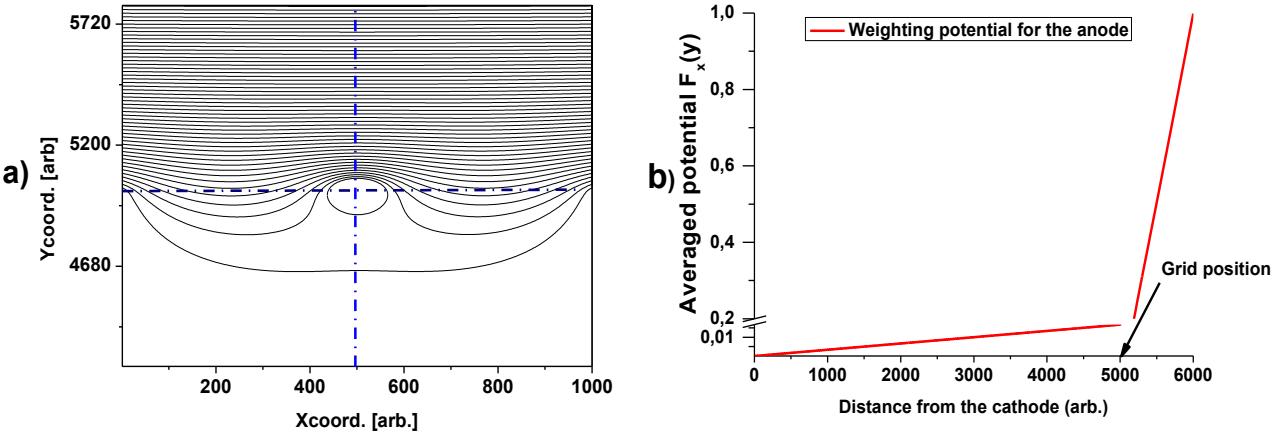

Figure 3. a) Weighting potential for the anode. b) Averaged weighting potential.

The path of the carrier must still be determined from the actual electric field. If the position of the carrier as a function of time is determined as previously described, then the time profile of the induced charge (or the induced current) can also be traced out to determine the shape of the output pulse. Calculation for gridded ionization chamber, shown in Fig.1, was done for a single cell with periodical boundary conditions in two dimensional Cartesian coordinates chosen as schematically shown in Fig. 2, where D and d are cathode-grid and grid-anode distances respectively. The boundary conditions (Dirichlet) for this case required us to specify the potential along the boundaries: anode potential set to 1, cathode and grids both grounded, potential along the dotted lines set to linear rising function of y coordinate from the zero at the cathode to 1 at the anode. The weighting potential (Fig. 3a) is found as the solution of Laplace equation $\frac{\partial^2 F(x,y)}{\partial x^2} + \frac{\partial^2 F(x,y)}{\partial y^2} = 0$.

The averaged potential as function of the distance between cathode and the anode of the chamber, presented in Fig. 3 band it was used for calculations of the anode pulses. The analytical equations for weighting potential Φ(x) could be written as follows:

$$\Phi(x)=\left\{\begin{array}{l}\dfrac{\sigma}{D},\ \text{when } 0\le \mathrm{x} < \mathrm{D}\\ \sigma+\dfrac{1-\mathrm{x}}{d}(x-D),\ \text{when } \mathrm{D}\le \mathrm{x} < \mathrm{D}+d\end{array}\right\} \tag{1}$$

Assuming the charge integrator was used as input of pulse processing apparatus, the total charge collected on the anode could be calculated as:

$$P_A=\int_0^L \rho(\xi)(1-\Phi(\xi\cos(\Theta))d\xi=[\text{using explicit values (1)}]=\mathrm{Ne}\cdot\left(1-\sigma\cdot\frac{\overline{\mathrm{X}}}{\mathrm{D}}\cdot\cos(\Theta)\right) \tag{2}$$

Similarly one could calculate the value of weighting potential at which the P_A reaches its half (this realizes when the center of ionization density distribution shifted to a point X between grid and anode with potential Φ(X)):

$$\frac{1}{2}\cdot P_A=\int_0^L \rho(\xi)\{\Phi_X-\sigma\cdot\frac{\xi}{D}\cdot\cos(\Theta)\}d\xi=Ne\cdot\left(\Phi_X-\sigma\cdot\frac{\overline{X}}{D}\cos(\Theta)\right) \tag{3}$$

From equation 3

$$\frac{1}{2}\cdot Ne\cdot\left(1-\sigma\frac{\overline{X}}{D}\cdot\cos(\Theta)\right)=\frac{1}{2}\cdot Ne\cdot\left(\Phi_X-\sigma\frac{\overline{X}}{D}\cdot\cos(\Theta)\right)\Rightarrow\Phi_X=\frac{1}{2}\cdot\left(1+\sigma\cdot\frac{\overline{X}}{D}\cos(\Theta)\right) \tag{4}$$

Recalling the assumption we made about the allocation of the center of ionization density distribution

$$X=D+\frac{d}{2}-\frac{\sigma}{(1-\sigma)}\cdot\frac{d}{2}\cdot\left(1-\frac{\overline{X}}{D}\cdot\cos(\Theta)\right) \tag{5}$$

Using eq. 5 the drift time necessary for center of ionization density distribution to take position at X:

$$T=\frac{D}{W}\cdot\left\{\left(1-\frac{\overline{X}}{D}\cdot\cos(\Theta)\right)+\frac{d}{2\cdot D}\cdot\left(1-\frac{\sigma}{1-\sigma}\cdot\left(1-\frac{\overline{X}}{D}\cos(\Theta)\right)\right\}\right. \tag{6}$$

From equation 6, introducing $T_0=T(\cos(\Theta)=1)$, $\mathrm{T}_{90}=T(\cos(\Theta)=0)$

$$T_{90}=\frac{D}{W}\cdot\left\{1+\frac{d}{2\cdot D}\cdot\left(1-\frac{\sigma}{1-\sigma}\right)\right\},\ T_0=\frac{D}{W}\cdot\left\{\left(1-\frac{\overline{X}}{D}\right)+\frac{d}{2\cdot D}\cdot\left(1-\frac{\sigma}{1-\sigma}\cdot\left(1-\frac{\overline{X}}{D}\right)\right\}\right. \tag{7}$$

Using above equation one derives:

$$\cos(\Theta)=\frac{T_{90}-T}{T_{90}-T_0},\ \text{and}\ \ \frac{\bar{X}}{D}\cdot\cos(\Theta)=(1-\frac{T}{T_{90}})\cdot(1+\frac{d}{2\cdot D-\sigma\cdot(2D-d)})\approx(1-\frac{T}{T_{90}})\cdot(1+\frac{d}{2\cdot D}) \qquad (8)$$

Finally for cosine and anode pulse height calculation we have got the formulae:

$$\begin{aligned} a)\quad & \cos(\Theta)=\frac{T_{90}-T}{T_{90}-T_0} \\ b)\quad & P_A^C=\frac{P_A}{1-\sigma(1-\frac{T}{T_{90}})\cdot(1+\frac{d}{2D})} \end{aligned} \qquad (9)$$

In 2E experiment with twin back-to-back ionization chamber (TBIC) two correlated fission fragment (FF) mass could be determined if their kinetic energies measured simultaneously along with their angles in respect to the chamber cathode plane [2]. FF angles usually necessary for corrections of their kinetic energies due to the loss in the target and target backing materials. There are two methods of FF angle determination one is the cathode pulse imitation by summing anode and grid signals, which recently carefully was investigated [3-5]. In this work we presented investigation of the second method, we will call drift time method. We implemented derived formulae to experiment recently carried out in Dubna using thermal neutron induced fission of ^{235}U of IBR-2 pulsed reactor. TBIC was operated at the following conditions: working gas P-10 with continuous flow of 50 ml/min at pressure of 1.08 bar, negative high voltage (-1750V) was applied to the common cathode, positive (+850V) to the anode and grounded grids. Grids were made of gilded tungsten of diameter 50 micron and spaced 2 mm from each other. Target was vacuum evaporated on the surface of gold plated (20 microgram/sq. cm) thin polyamide backing (of 35 microgram/sq. cm) obtained from EC-JRC-IRMM. The electrodes of TBIC have circular shape of diameter 160 mm. Target was mounted at the center of the cathode and had circular shape of 70 mm. The distance between cathode and grid was chosen D=40 mm and the distance between grid and anode d= 10 mm. Measurements was done using six channel synchronized waveform digitizers Mi-3242 from SPECTRUM-INSTRUMENTATION company (Sampling rate 250MHz, Resolution 12 bit). The detailed description of data acquisition systems and digital pulse processing (DPP) algorithms provided in separate poster of this conference. In this presentation we have analyzed list mode data obtained after DPP applied to waveforms acquired during measurements. Our goal was to demonstrate the result of analysis with use of formulae (9), derived above.

After cosines measured the pulse heights were corrected for grid inefficiency according to formula 9b and, then two plots generated as shown in Fig. 4. In left figure two dimensional plot in coordinates $\cos(\Theta_1)$, $\cos(\Theta_2)$ generated for full set of events, in right figure plot was generated only for events with average cosine value greater than 0.5. It is clear that the cosine accuracy is better than 0.056. In Fig.5 two-dimensional plots of the $Y(P_A^C,\cos(\Theta))$ function are measured and plotted for two sides of TBIC. These plots were used for energy loss correction in both sides of the target. Kinetic energy loss depended on thickness of target or backing material, which FF pass to enter the TBIC sensitive volume. If the compositions of target and backing were homogeneous, then the energy losses are proportional to inverse value of $\cos(\Theta)$ measured in corresponding chamber.

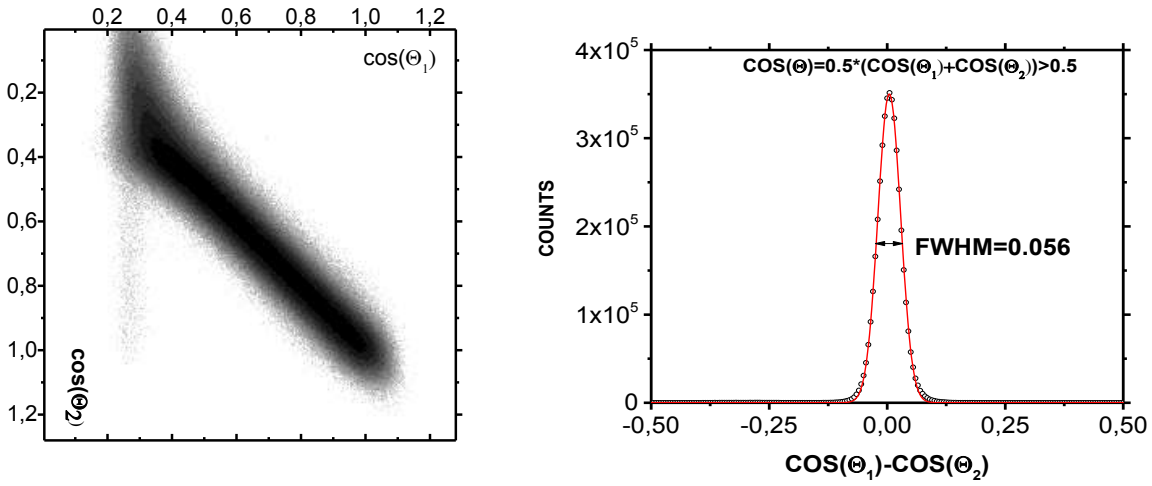

Figure 4. Two dimensional plots (left graph, logarithmic scale) of simultaneously measured cosines in both sides of TBIC made using formula (9a). In the right graph difference between simultaneously measured cosines is plotted, demonstrating the accuracy of cosine measurement.

The scaling factor of proportionality is the measure of the energy losses in the target and the layer. To find these values for both sides of one have to find the "center of gravity" of one-dimensional distributions calculated for fixed cosine values of $\mathrm{Y}(P_A^C, \cos(\Theta) = const)$:

$$P_{CG}(\cos(\Theta) = const) = \frac{\int_{P_0}^{P_{\max}} Y(P_A^C, \cos(\Theta) = const) \cdot P_A^C \cdot dP_A^C}{\int_{P_0}^{P_{\max}} Y(P_A^C, \cos(\Theta) = const) \cdot dP_A^C} \tag{10}$$

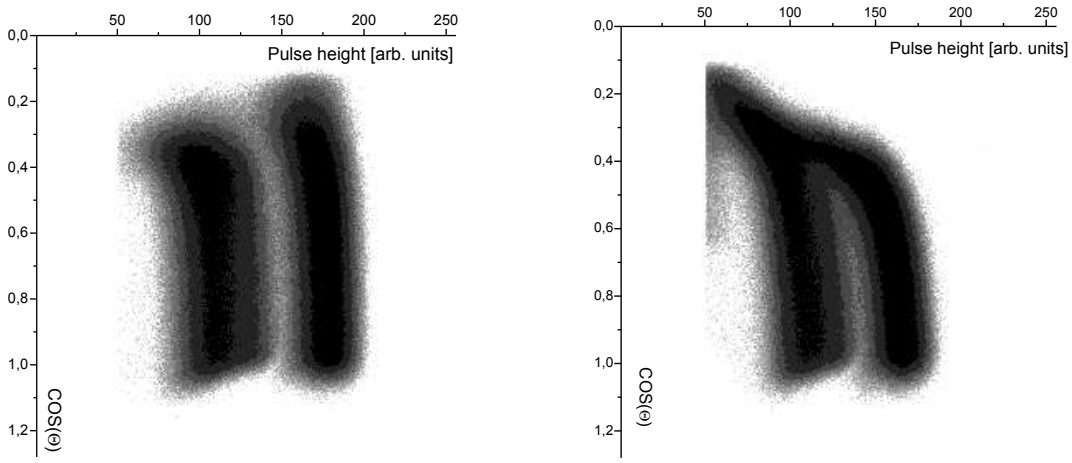

Figure 5. Two-dimensional plot of pulse height, cos(Θ) for the layer side (left) and for the backing side (right).

Then the calculated values should be plotted versus reverse cosine value as shown in Fig. 6 and fitted by linear function. The value Δ of the tangent of fitted function was assigned the scaling factor and can be used for energy losses correction using the following formula:

$$P = P_A^C + \Delta / \cos(\Theta) \tag{11}$$

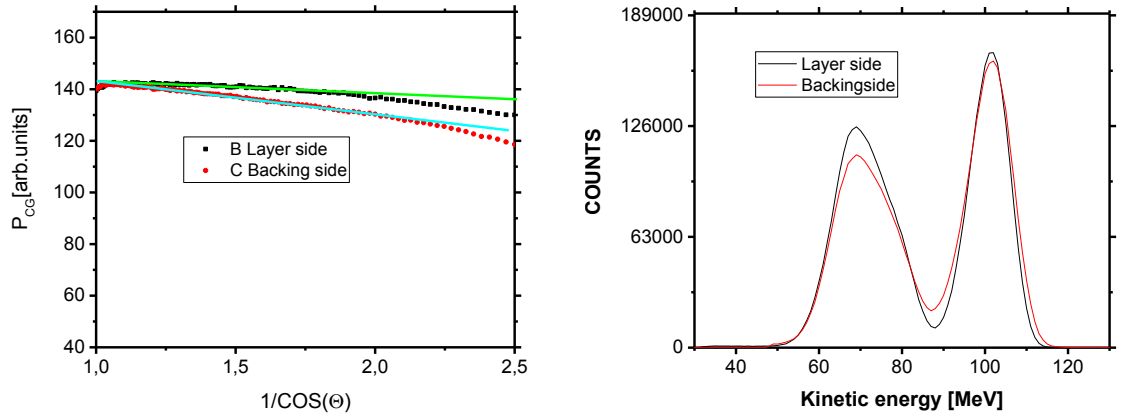

Figure 6. Two-dimensional plot of pulse height versus cos(Θ) for the layer side (left) and for the backing side (on the left figure). FF kinetic energy distributions after correction for energy losses in the layer and backing applied.

References

1. G.F. Knoll, Radiation detection and measurements, New York: Wiley, 2000.
2. C. Budtz-Jørgensen and H.-H. Knitter, *Nucl. Inst. and Meth.*, A **258**, 307 (1987).
3. A. Al-Adili, F.-J. Hambsch, R. Bencardino, S. Oberstedt, S. Pomp. S. Zeynalov. NIMA **671** (2012) 103–107.
4. A. Gook, F.-J. Hambsch, A. Oberstedt, S. Oberstedt. NIMA **664** (2012) 289–293.
5. A. Gook, Investigation of the Frisch-grid inefficiency by means of wave-form digitization, Orebro Universitet, 2008-06-23.